ChemistrySelect

Research Article
doi.org/10.1002/slct.202304783

Chemistry Europe
European Chemical Societies Publishing

www.chemistryselect.org

# Novel Pyrazole Derivatives Bearing Carbonitrile and Substituted Thiazole Moiety for Selective COX-2 Inhibition

Ege Arzuk,[a] Fuat Karakuş,[b] Ali Ergüç,[c] and Burak Kuzu*[d]

In this study, a series of derivatives of pyrazole hybrid structures containing carbonitrile and substituted thiazole moiety were designed to search for selective COX-2 inhibition. The designed target structures were synthesized with easy, practical, and efficient procedures. COX-1/2 inhibition and cytotoxic effects of the synthesized compounds were evaluated in NIH/3T3 and MDA-MD-231 cell lines for inhibition concentration and selectivity index. The results showed that the compounds have an inhibitory effect with higher selectivity towards COX-2 overall in both cell lines and moderate antiproliferative activity by targeting the breast cancer cell line MDA-MB-231. Among the 19 compounds synthesized (**19a–t**), especially compound **19m** was found to be highly effective with COX-2 inhibition of 5.63 μM in the NIH/3T3 cell line and 4.12 μM in the MDA-MB-231 cell line. Moreover, molecular docking studies showed that the compounds indeed exhibited higher affinity for the COX-2 active site. The theoretical ADMET properties of the presented compounds were calculated, and the results showed that the compounds may have a more favorable pharmacokinetic effect profile than the selective COX-2 inhibitor Celecoxib, thus promising COX-2 inhibitor drug candidates for the future.

## Introduction

Prostaglandin-endoperoxidase synthase (PTGS), commonly identified as cyclooxygenase (COX), catalyzes reactions that lead to the formation of prostaglandin and related compounds from arachidonic acid.[1] So far, three different isoforms of the COX enzyme, COX-1, COX-2, and COX-3 have been characterized. The COX-1 enzyme is produced under normal physiological conditions where it is responsible for prostaglandin synthesis and has a cytoprotective effect by regulating platelet activity, kidney, and stomach functions.[2] COX-2 is induced due to inflammatory stimuli and is usually found in cells with increased prostaglandin levels during inflammatory reactions.[3] The most recently discovered enzyme, COX-3, is mostly found in the spinal cord and brain.[4]

NSAIDs targeting the commonly found COX-1 and COX-2 enzymes exert anti-inflammatory effects by selective/non-selective inhibition of COX activity and subsequently block the biosynthesis of prostaglandins at lesion sites.[5–7] However, non-selective NSAIDs that provide simultaneous inhibition of COX-1 and COX-2 not only achieve anti-inflammatory and analgesic purposes but also cause serious side effects such as gastrointestinal damage and platelet dysfunction. While selective COX-2 inhibitor NSAIDs only inhibit COX-2, they do not affect the protective effect of COX-1-catalyzed prostaglandins on the gastrointestinal tract and platelets, thus greatly reducing the risk of gastrointestinal side effects.[7,8] Although selective COX-2 inhibitors are the most common treatment option for inflammatory diseases, they have often been associated with potential side effects of cardiovascular disorder, possible heart attack, blood clots, and increased risk of stroke. Therefore, discovering new and selective COX-2 inhibitors that can reduce such side effects is becoming increasingly important.[9,10] For example, during the COVID-19 pandemic, COX-2 inhibitors have been the groups of drugs that are urgently applied. The coronavirus disease (COVID-19) is based on infection with the severe acute respiratory syndrome coronavirus.[11,12] Unfortunately, the desired result could not be achieved with the use of existing potential prophylactic and therapeutic intervention drugs for rapid response to the disease during the pandemic. However, during the (severe) infection of SARS-CoV-2, an important inflammatory disease, the use of various cyclooxygenase (COX) inhibitors has led to some desirable successes.[13,14]

Celecoxib, which has a very high COX-2 selectivity, is a heterocyclic compound containing a pyrazole ring, and various pharmaceuticals are produced by derivatizing the pyrazole moiety in its structure. The important route followed in the development of more effective COX-2 inhibitor and anti-inflammatory drug candidates is compound derivatives developed by modifications of functional groups in the Celecoxib. For example, it has been reported that compound **1**, developed by replacing the sulfonyl amide group in Celecoxib with the cyano group, exhibits as effective inhibition potential as

[a] *Dr. E. Arzuk*
*Department of Pharmaceutical Toxicology, Faculty of Pharmacy, Ege University, İzmir, 35040, Türkiye*
*E-mail: ege.arzuk@ege.edu.tr*

[b] *Dr. F. Karakuş*
*Department of Pharmaceutical Toxicology, Faculty of Pharmacy, Van Yuzuncu Yil University, Van, 65080, Türkiye*
*E-mail: fuatkarakus@yyu.edu.tr*

[c] *Dr. A. Ergüç*
*Department of Pharmaceutical Toxicology, Faculty of Pharmacy, İzmir Kâtip Çelebi University, İzmir, 35620, Türkiye*
*E-mail: alierg33@gmail.com*

[d] *Dr. B. Kuzu*
*Department of Pharmaceutical Chemistry, Faculty of Pharmacy, Van Yuzuncu Yil University, Van, 65080, Türkiye*
*E-mail: burakkuzu@yyu.edu.tr*

*Supporting information for this article is available on the WWW under https://doi.org/10.1002/slct.202304783*

selective COX-2 inhibitors ($IC_{50}$: 7.07 μM).[15] A similarly designed diaryl pyrazole derivative compound **2** ($IC_{50}$: 1.11 μM) was found to exhibit COX-2 inhibition similar to Celecoxib ($IC_{50}$: 0.87 μM) by the addition of the methylsulfonyl group.[16] Compound **3** ($ED_{50}$: 0.98 μM), which carries a thiazole group in the pyrazole ring system, is more effective than the reference compounds Celecoxib ($ED_{50}$: 1.54 μM) and meclofenamate sodium ($ED_{50}$: 5.64) in *in vivo* studies (Figure 1).[17]

In addition, Razik et al. studied the dual inhibition of COX (COX-1 and COX-2) and 5-LOX (5-lipoxygenase) by designing benzodioxol-pyrazole hybrids containing a new type of thiazolone derivative. *In vitro* studies revealed that compound **4** (COX-2 $IC_{50}$: 0.33 μM, Selectivity Index = 12.06) is a more potent derivative than Celecoxib (COX-2 $IC_{50}$ = 0.88 μM).[18] In another study, the $-CF_3$ substituted pyrazole derivative compound **5** exhibited COX-2 inhibition by the standard drugs diclofenac sodium ($IC_{50}$: 3.1 μM, $ED_{50}$: 87.3 mg/kg) and Celecoxib ($IC_{50}$: 0.28 μM, $ED_{50}$: 200 mg/kg).[19] The trisubstituted pyrazole derivative compound **6**, high COX-2 selectivity (SI: 9.87), and moderate anti-inflammatory potential ($ED_{50}$: 15.06 mol/kg) effect was determined by comparison with Celecoxib (SI: 8.61 and $ED_{50}$: 82.2 mol/kg). In docking studies (PDB ID: 3LN1), it was discovered that the hydrazone nitrogen in the fourth position of the pyrazole ring has important binding interactions for COX-2 selectivity.[20]

El-Shukrofy et al. synthesized pyrazole derivatives containing thienopyrimidine, thienotriazolopyrimidine, and thiophene groups and investigated their *in vitro* COX-1/COX-2 inhibition and *in vivo* anti-inflammatory activities. The results showed that the thienopyrimidine derivative compound **7** is a potent COX-2 inhibitor. Based on *in vitro* studies, the COX-2 inhibition and selectivity index ($IC_{50}$ = 0.059 μM and SI = 190.34) of compound **7** was comparable to Celecoxib ($IC_{50}$ = 0.045 μM and SI = 326.67) as the reference drug indomethacin ($IC_{50}$ = 0.080 μM and SI = 1.25).[21] Again, compound **8**, one of the trisubstituted pyrazole derivatives developed for COX-2 activity, has a thiadiazol structure as a quintuple heterocyclic structure at the 4th position of the pyrazole ring. It was discovered that compound **8** had a higher inhibition of 87.25% of the COX-2 activity studied with the reference compound diclofenac sodium (86.72%).[22] Despite the absence of *p*-sulfonyl amide phenyl group in the 1st position of the pyrazole ring in both compounds, it is seen that the COX-2 selective activity continues in the compounds.

Inceler et al. synthesized new pyrazole derivatives with two aryl rings and investigated the in vitro COX-2 inhibition of these derivatives. Here, compound **9** was reported to be the strongest inhibitor with 84.27% COX-2 inhibition compared to indomethacin (66.27%) as the standard drug.[23] Also, Tageldin et al. designed and synthesized new pyrazolopyrimidine derivatives by substituting different functional groups on the pyrazole ring. In the *in vitro* COX-2 inhibition assessment of the series, compound **10** was the most potent compound with $IC_{50}$ = 0.22 μM and SI = 12.45, compared to reference Celecoxib (COX-2 $IC_{50}$ = 0.78 μM and SI = 7.23).[24] A new class of cyanopyridone-substituted pyrazole derivatives (compound **11**) has been developed by enclosing the nitrogen atom in the 4th position of the pyrazole ring. It has been observed that the anti-inflammatory effect of this developed structure with indomethacin (72.99%) and Celecoxib (83.76%) drugs is quite remarkable with 89.57% (Figure 2).[25]

Based on this summary of the literature, new selective COX-2 inhibitors can be developed with effective molecular modifications of compounds designed according to the Celecoxib molecule. Relevant molecular modifications can be summarized as follows; *i*: aromatic or heteroaromatic group at 1st position of the pyrazole ring, *ii*: substituted phenyl groups at 3rd position, and *iii*: a $sp^2$ hybridized nitrogen (a carbon atom away from pyrazole) at 4th position. These features are schematized as a literature model in Figure 3. We designed new class pyrazole derivatives containing carbonitrile and substituted thiazole according to this molecular topology which we suggested in this study. In the molecular design, there is a substituted thiazole group in the 1st position of the pyrazole ring, substituted aromatic groups in the 3rd position, and a carbonitrile group in the 4th position, which ensures that it contains a nitrogen atom one carbon atom away from pyrazole ring.

So, we designed and synthesized 19 different pyrazole hybrid derivatives to evaluate COX-1/2 inhibition activity in the non-tumorogenic and tumorogenic cell lines (3NIH/3T3 and MDA-MB-231 respectively) compared to the COX-2 inhibitor Celecoxib. We also evaluated the target compounds' structure-activity relationship (SAR), molecular docking studies for COX-1/2 enzymes, and some theoretical pharmacokinetic properties.

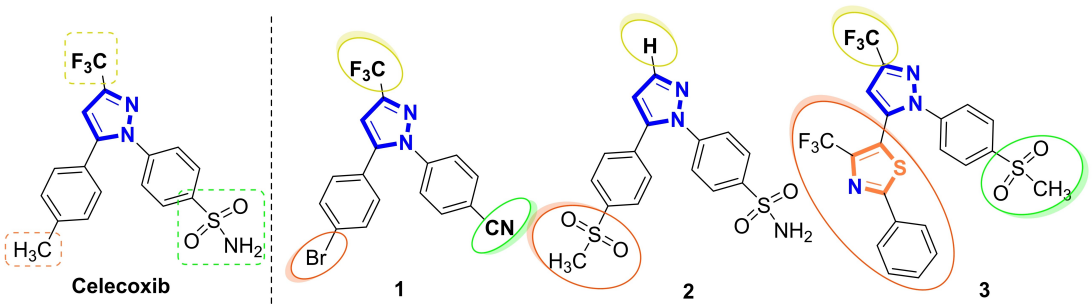


**Figure 1.** Celecoxib and its modified derivatives.

Research Article
doi.org/10.1002/slct.202304783
Chemistry Europe
European Chemical Societies Publishing

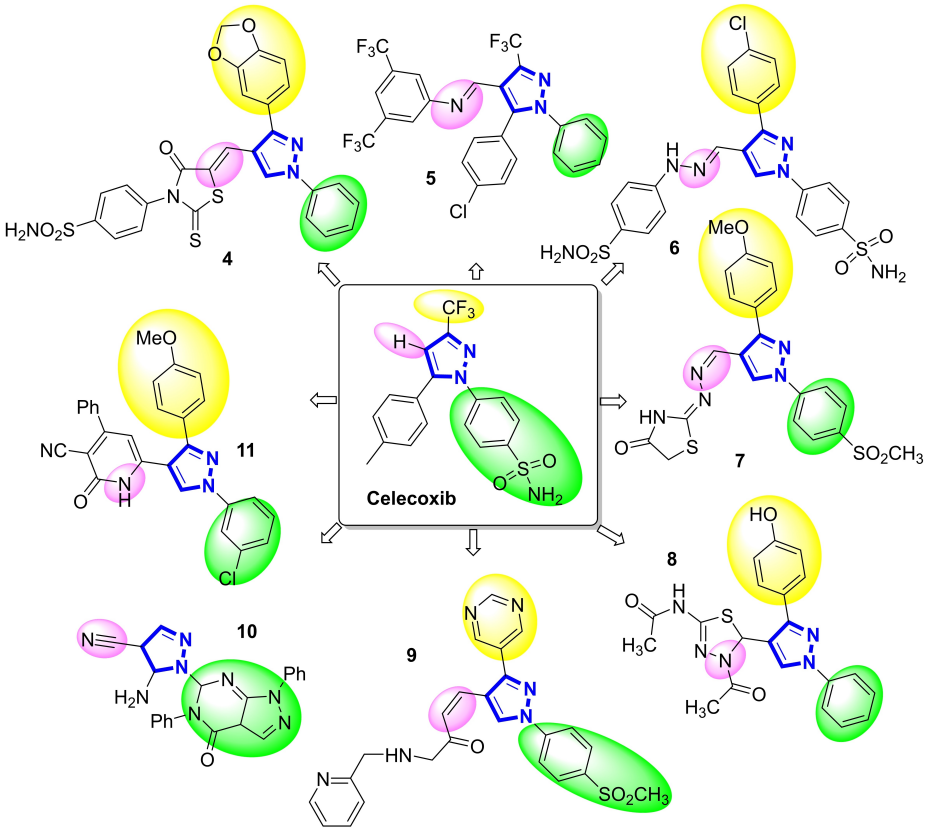


**Figure 2.** Selective COX-2 inhibitor pyrazole derivatives derived from Celecoxib.

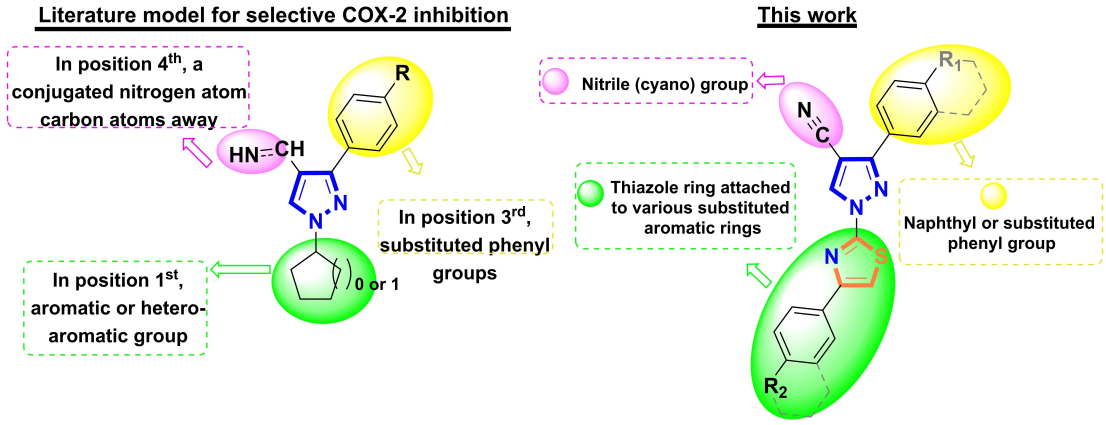


**Figure 3.** Literature model for COX-2 inhibition and the designed target compounds.

## Results and Discussion

### Chemistry

The synthetic approach adopted to afford the target compounds Scheme 1. Initially, the conversion of substituted acetophenone compounds (**12a–j**) with thiosemicarbazide (**13**) to thiosemicarbazone (**14a–j**) and their next step reactions with alpha-bromo acetophenone reagents (**15k–t**) to thiazole hydrazone derivatives (**16a–t**) were prepared according to our previous work.[26] The compounds (**16a–t**) obtained after the mentioned step were heated under Vilsmeier-Haack conditions ($POCl_3$, DMF) at 80 °C for 1 h., and then the target compounds (**17a–t**) were synthesized with high yield by neutralization. Finally, the conversion of the carbaldehyde group to the oxime (**18a–t**) followed by the nitrile group was carried out in a two-step reaction to obtain the target compounds **19a–t**.

NMR and elemental analysis data supported the success of the applied route. $^1$H NMR of all target compounds showed single characteristic signals for aromatic proton in the pyrazole ring detected as single signals at δ: 8.85–9.66 ppm. Besides, all compounds' expected aromatic and aliphatic protons were

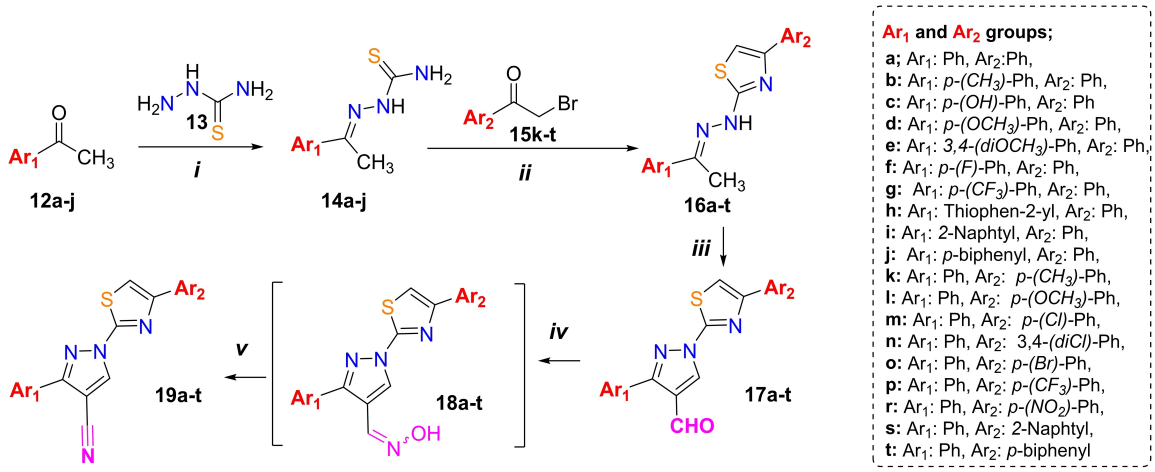


**Scheme 1.** The total synthesis scheme of target compounds, *i*: EtOH, Reflux, 4 h. *ii*: EtOH, Reflux, 1 h. *iii*: DMF, $POCl_3$, 80 °C, 3 h. *iv*: 1-PrOH, $NH_2OH.HCl$, 3 h. v: Acetic anhydride, 1 h.

detected in the $^1$H-NMR spectrums. In addition, the C-3 signals of the pyrazole ring in the range of δ: 154.7–169.1 ppm were observed in the $^{13}$C-NMR spectrum. All other $^{13}$C-NMR spectrum signals were matched to the type and number of carbons in the compounds (see Supp. Info.).

## Biological Evaluation

In recent years, COX-2 has emerged as a crucial target in anti-cancer therapy, with a particular focus on Celecoxib and its derivatives and their anti-cancer potential, especially in breast cancer.[27] Given COX-2's overexpression in cancer, the study evaluated the COX activities of newly synthesized pyrazole derivatives (**19a–t**) on both MDA-MB-231 and NIH/3T3 cells using the MTT assay. The $IC_{50}$ values were determined using GraphPad's non-linear regression approach for log (inhibitor) vs. normalized response-variable slope was used to determine $IC_{50}$ values [$Y = 100/(1 + 10(X–LogIC_{50})$. Results indicated low toxicity to healthy cells but significant cytotoxicity against breast cancer cells for most compounds. MDA-MB-231 cells showed high sensitivity, with selectivity values above 2 (Table 1).

## Structure-Activity Relationship (SAR)

In the MTT results of the synthesized compounds in the MDA-MB-231 cell line, it is seen that especially the compound **19c** stands out. It can be deduced that the 4-hydroxyphenyl substituted compound **19c** is the antiproliferative agent with the highest potency in the MDA-MB-231 cell line with an $IC_{50}$: 42 ± 0.73 μM and SI: 7.11. The 3,4-dimethoxy substituted compound **19e**, which gives the closest result similar to this result, has $IC_{50}$: 65.3 ± 0.83 μM and SI: 4.58. The remaining compounds have antiproliferative effects close to each other in the range of $IC_{50}$: 60–100 μM and SI: 2.8–4.49 values (Table 1).

**Table 1.** $IC_{50}$ values of the compounds and Celecoxib in healthy (NIH/3T3) and cancer cells (MDA-MB-231).

| | $IC_{50}$ (μM) | | |
|---|---|---|---|
| *Compounds* | NIH/3T3 | MDA-MB-321 | Selectivity index* |
| Celecoxib | 264.3 ± 0.36 | 25.2 ± 0.41 | 10.49 |
| 19a | 274.3 ± 0.73 | 61.1 ± 0.52 | 4.49 |
| 19b | 197.5 ± 0.78 | 71.2 ± 1.01 | 2.77 |
| **19c** | 298.6 ± 0.84 | 42 ± 0.73 | 7.11 |
| 19d | 242.7 ± 0.89 | 65.8 ± 0.14 | 3.69 |
| **19e** | 299.4 ± 1.8 | 65.3 ± 0.83 | 4.58 |
| 19f | 293.4 ± 0.09 | 71.4 ± 0.45 | 4.11 |
| 19g | 267.6 ± 1.02 | 69.6 ± 0.28 | 3.84 |
| 19h | 226.4 ± 0.28 | 73.5 ± 0.23 | 3.08 |
| 19i | 269.8 ± 0.35 | 64.8 ± 0.51 | 4.16 |
| 19j | 264.5 ± 0.97 | 59.8 ± 0.46 | 4.42 |
| 19k | 243.7 ± 0.73 | 61.91 ± 0.77 | 3.94 |
| 19l | 279.2 ± 0.4 | 71.75 ± 0.29 | 3.89 |
| 19m | 265.2 ± 0.29 | 73.1 ± 0.03 | 3.63 |
| 19n | 282.4 ± 1.03 | > 100 | > 2.8 |
| 19o | 242.5 ± 1.08 | 65.32 ± 0.53 | 3.71 |
| 19p | 282.1 ± 0.72 | 65.4 ± 0.52 | 4.30 |
| 19r | 289.7 ± 0.73 | > 100 | > 2.9 |
| 19s | 263.3 ± 0.63 | > 100 | > 2.6 |
| 19t | 295.9 ± 0.18 | > 100 | > 3 |

COX-1 inhibition was absent, while the potential for COX-2 inhibition (with a cut-off value of ≤ 5 μM[28]) varied. Compounds **19d**, **19e**, **19l**, and **19m** demonstrated specific COX-2 inhibition, with selectivity indexes of 31.57, 30.6, 31.09, and 48.99, respectively (Table 2 and Table 3).

Compounds **19c** (30.17), **19d** (SI: 29.71), **19e** (24.85), **19m** (SI: 37.70), and **19l** (32.14) appear to have a higher inhibition profile for COX-2 in the NIH/3T3 healthy cell line (Table 2). Accordingly, it can be concluded that 4-OH-phenyl (**19c**), 4-

**Table 2.** COX-1 and COX-2 inhibition potential of compounds on NIH/3T3 cells.

| Compounds | $IC_{50}$s in NIH/3T3 | | |
|---|---|---|---|
| | COX-1 (μM) | COX-2 (μM) | Selectivity index |
| Celecoxib | 174.7 ± 0.071 | 0.535 ± 0.002 | 326.54 |
| 19a | 142.05 ± 0.125 | 16.541 ± 1.05 | 8.59 |
| 19b | 83.6 ± 1.091 | 5.3 ± 0.449 | 15.77 |
| **19c** | 196.5 ± 0.51 | 6.513 ± 1.02 | 30.17 |
| **19d** | 156.2 ± 0.534 | 5.258 ± 0.131 | 29.71 |
| **19e** | 142.3 ± 0.82 | 5.726 ± 0.621 | 24.85 |
| 19f | 163.5 ± 0.553 | 20.6 ± 0.173 | 7.94 |
| 19g | 105.9 ± 0.937 | 5.26 ± 0.08 | 20.13 |
| 19h | 189.6 ± 1.156 | 218.8 ± 0.186 | 0.87 |
| 19i | 216.8 ± 0.121 | 206.5 ± 1.05 | 1.05 |
| 19j | 136.5 ± 0.75 | 140.3 ± 0.283 | 0.97 |
| 19k | 172.9 ± 1.09 | 20.8 ± 0.0715 | 8.31 |
| **19l** | 226.8 ± 0.004 | 7.056 ± 0.375 | 32.14 |
| **19m** | 212.3 ± 0.319 | 5.632 ± 0.42 | 37.70 |
| 19n | 160.2 ± 0.061 | 172.5 ± 0.108 | 0.93 |
| 19o | 628.6 ± 0.385 | 589.6 ± 1.035 | 1.07 |
| 19p | 152.6 ± 0.439 | 8.6 ± 0.153 | 17.74 |
| 19r | 403.8 ± 1.027 | 512.9 ± 0.091 | 0.79 |
| 19s | 183.5 ± 1.005 | 116.05 ± 1.18 | 1.58 |
| 19t | 215.6 ± 1.15 | 102.8 ± 0.098 | 2.10 |

**Table 3.** COX-1 and COX-2 inhibition potential of compounds on MDA-MB-321 cells.

| Compounds | $IC_{50}$s in MDA-MB-321 | | |
|---|---|---|---|
| | COX-1 (μM) | COX-2 (μM) | Selectivity index |
| Celecoxib | 193.6 ± 0.052 | 0.142 ± 0.015 | 1363.38 |
| 19a | 158.09 ± 0.006 | 13.3 ± 1.23 | 11.89 |
| 19b | 156.9 ± 1.006 | 7.6 ± 1.261 | 20.64 |
| 19c | 150.2 ± 0.148 | 5.62 ± 0.82 | 26.73 |
| **19d** | 141.4 ± 0.612 | **4.415 ± 0.082** | **31.57** |
| **19e** | 138.5 ± 0.526 | **4.526 ± 0.423** | **30.60** |
| 19f | 152.6 ± 0.856 | 18.8 ± 0.253 | 8.12 |
| 19 g | 146.2 ± 0.402 | 7.32 ± 0.153 | 19.97 |
| 19 h | 206.5 ± 0.964 | 236.9 ± 0.102 | 0.87 |
| 19i | 242.3 ± 0.268 | 224.7 ± 1.26 | 1.08 |
| 19j | 196.5 ± 0.82 | 128.5 ± 0.956 | 1.53 |
| 19k | 185.7 ± 1.12 | 19.4 ± 0.146 | 9.57 |
| **19l** | 202.9 ± 0.052 | **6.526 ± 0.762** | **31.09** |
| **19m** | 202.1 ± 0.808 | **4.125 ± 0.96** | **48.99** |
| 19n | 149.8 ± 0.461 | 143.9 ± 1.54 | 1.04 |
| 19o | 513.5 ± 0.846 | 402.8 ± 1.15 | 1.27 |
| 19p | 148.0 ± 0.263 | 6.46 ± 0.826 | 22.91 |
| 19r | 558.9 ± 0.422 | 622.3 ± 1.012 | 0.90 |
| 19 s | 264,3 ± 0.015 | 159.26 ± 1.06 | 1.66 |
| 19 t | 245.7 ± 1.06 | 163.7 ± 0.085 | 1.56 |

OMe-phenyl (**19d**), 3,4-diOMe-phenyl (**19e**), and substituents in the $Ar_1$ group; 4-Cl-phenyl (**19m**) and 4-OMe-phenyl (**19l**) substituted compounds in the $Ar_2$ group, have higher COX-2 selectivity (Table 2).

A similar result is observed when the inhibition profile of the compounds on the COX-1/2 enzyme in the MDA-MB-231 cancer cell line is examined. It turns out that **19d**, **19e**, **19m**, and **19l** structures are the compounds with the highest COX-2 selectivity with selectivity indexes of 31.57, 30.6, 48.99, and 31.09 respectively (Table 3). In addition, it is seen that the COX-2 selectivity of compounds bearing 4-hydroxyphenyl, 4-methoxyphenyl, or 3,4-dimethoxyphenyl groups in the $Ar_1$ ring and 4-chlorophenyl and 4-methoxyphenyl substituted compounds in $Ar_2$ is higher than the other compounds (Figure 4). According to this data, electron-donating groups in both $Ar_1$ and $Ar_2$ groups increase COX-2 selectivity for both cell lines.

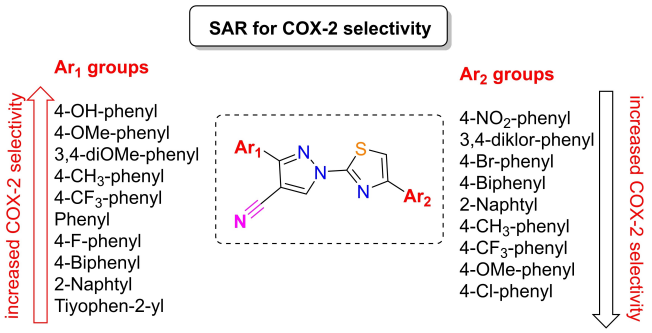


**Figure 4.** SAR of the synthesized compounds on COX-2 selectivity.

## Molecular Docking Studies

Crystal structures with Celecoxib as an inhibitor ligand in the active site of COX-2 enzyme obtained from the protein data bank. The active site was determined by simulating the complex binding modes of this inhibitor, and docking studies were done under validated conditions. The docking scores of the compounds **9d**, **9e**, **9m**, and **9l**, in the active site of COX-2 enzyme are presented in Table 4.

Compounds **19d**, **19e**, **19l**, and **19m** come to the fore as a result of inhibition studies on the COX-2 enzyme of 19 different synthesized new derivatives. The interaction potentials of the selected compounds in the COX-2 active site have lower binding potential than the Celecoxib control inhibitor ligand, which supports *in vitro* studies. However, **19d**, **19e**, **19m**, and **19l** compounds make H-bond interactions with Arg 499, non-covalent interaction with Tyr341, and Val509 residues in the COX-2 active site like Celecoxib. *In vitro* tests and molecular docking studies show that the most potential compound for COX-2 inhibition is **19m**. It can be said that the compound **19m** forms a complex by interacting with other residues in the COX-2 active site with a Celecoxib-like position (Figure 5 and Figure 6).

**Table 4.** The docking scores of the compounds **19a–t** against human COX-2 enzyme.

| Comp. | Crystal Structure of Celecoxib bound at the COX-2 active site (PDB ID: 3LN1) | | | |
|---|---|---|---|---|
| | Binding Energy (kcal/mol) | Cluster RMSD (Å) | H-bonding | Other non-covalent interactions |
| Celecoxib | −11.31 | 0.10 | His75, Arg499, Ile503, Phe504 | Val335, Ser339, Tyr341, Leu345, Leu370, Trp373, Met508, Val509, Gly512, Ala513 |
| **19d** | −9.67 | 0.12 | Arg499 | Leu338, Ser339, Tyr341, Leu370, Trp373, Asp501, Ala502, Phe504, Met508, Val509, Gly512 |
| **19e** | −9.28 | 0.16 | Arg499 | His75, Leu338, Tyr341, Leu370, Tyr371, Asp501, Ala502, Phe504, Val509, Gly512 |
| **19l** | −9.35 | 0.15 | Arg499 | Tyr341, Ala502, Phe504, Val509, Ala513, Asp501 |
| **19m** | −9.89 | 0.13 | Arg499 | His75, Val335, Tyr341, Asp501, Ala502, Val509, Ala513. |

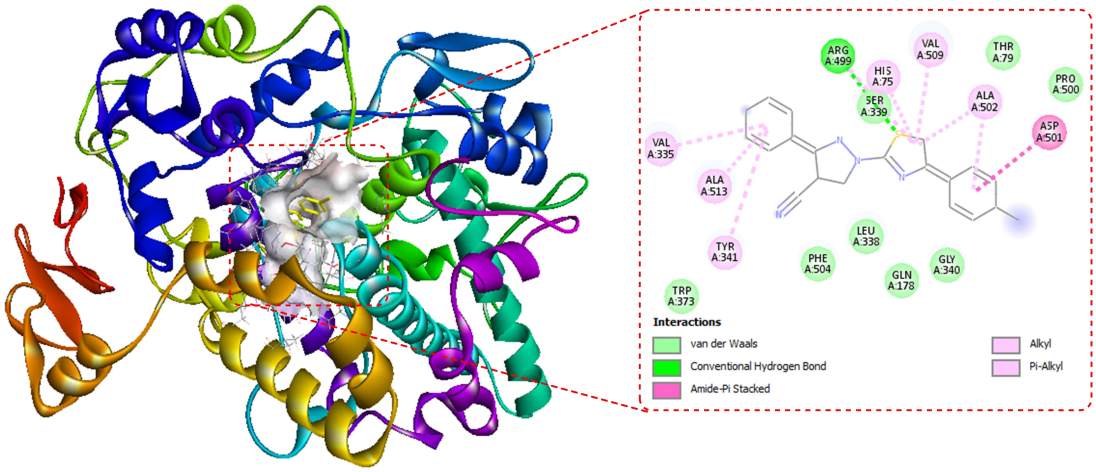


**Figure 5.** 3D and 2D ligand-protein interactions of COX-2 active site with compound 19 m.

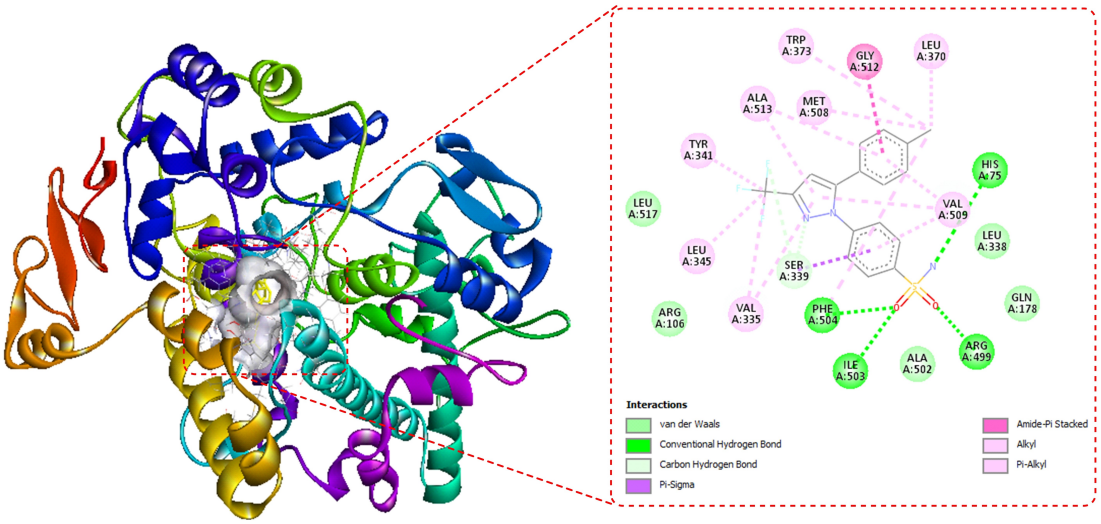


**Figure 6.** 3D and 2D ligand-protein interactions of COX-2 active site with Celecoxib.

### The drug-likeness and theoretical pharmacokinetic parameters of target compounds

Hepatotoxicity and cardiotoxicity are key factors leading to drug failure in both pre-clinical and clinical stages, as well as the withdrawal of drugs from the pharmaceutical market. Therefore, human hepatotoxicity, cardiotoxicity, and certain ADME parameters were evaluated with the ADMETlab 2.0 web tool and presented in Table 4. Analysis of toxicity results revealed that the hit compounds had a lower probability of blocking hERG (—) compared to Celecoxib (–), and **19d** and **19e** exhibited no hepatotoxicity. Conversely, **19l** and **19m** showed higher hepatotoxicity potential than Celecoxib. Despite a higher maximum recommended daily dose, absorption from the human intestine was comparable between the hit compounds and Celecoxib.

Since a large part of Celecoxib is metabolized in the liver by CYP 2C9,[29] the CYP 2C9 inhibition potential of the compounds was also evaluated, and the potency of compound **19d** was equal to that of Celecoxib. The hit compounds exhibited moderate clearance (5–15 mL/min/kg) compared to Celecoxib's poor clearance. Finally, all four hit compounds complied with Lipinski's rules. While Celecoxib, a selective COX-2 inhibitor, displayed a superior $IC_{50}$ ($0.142 \pm 0.015$, Table 2), **19d** and **19e** showed advantages over Celecoxib, particularly in terms of toxicity (Table 5).

## Conclusions

In this study, a literature model for COX-2 inhibition was created by investigating new heterocyclic compounds derived from Celecoxib and their activities in the literature. According to this model, a series of trisubstituted pyrazole structures containing carbonitrile, substituted aryl, and thiazole moieties were designed and synthesized. It was found that 19 newly synthesized hybrid compounds were antiproliferative for the estrogen-positive (ER+) breast cancer cell line MDA-MB-231 in MTT results and had a selective inhibition profile for COX-2 in this cell line. In the SAR study established for COX-2 inhibition, it was observed that electron-donating substituents in the $Ar_1$ and $Ar_2$ groups positively increased COX-2 inhibition. It has been supported by molecular docking studies that the prominent compounds **19d**, **19e**, **19l**, and **19m** can form a complex with a Celecoxib-like interaction in the COX-2 active site. Additionally, the theoretical pharmacokinetic properties of the mentioned compounds showed that they have less toxic effect potential and more drug-like properties than Celecoxib. The results indicate that the compounds presented here may be promising drug candidates for COX-2 inhibition and pioneers in the development of new COX-2 inhibitory compounds.

## Experimental Section

### Chemistry

**General Information**. $^1H$ and $^{13}C$ NMR spectra were recorded on a Varian-Agilent Inova instrument (400 and 100 MHz, respectively) using $Me_4Si$ (TMS) as the internal standard. Melting points were determined on a Stuart Melting Point (SMP30) analyzer using open glass capillaries. Column chromatography was performed on silica gel (60 mesh, Silycycle). Commercially available materials were used without further purification. The analyses of the C, H, and N elements of the compounds were made with the LECO 932 CHNS (St. Joseph, MI, USA) elemental analysis device. Analysis results have a maximum deviation of $\pm 0.4$ from the calculated theoretical values.

**Synthesis of compounds 14a–j**. Initially, 5 mmol acetophenone derivatives (**5a–j**) were dissolved/suspended in ethanol (10 mL) and magnetically stirred with 6 mmol thiosemicarbazide (**13**). The reaction mixture was refluxed at 70 °C for 8–16 h., and the completion of the reaction was checked by TLC. Afterward, the experiment was terminated and cooled to room temperature, and the formed particles were filtered out. Solid particles washed several times with distilled water were allowed to dry at room temperature. The obtained thiosemicarbazone derivatives (**14a–j**) were used for the next step without further purification.[30]

**Synthesis of compounds 16a–t**. 4 mmol thiosemicarbazone derivatives (**14a–j**) obtained in the previous step were dissolved in 10 ml of ethanol by heating. Reflux was made for 1 h by adding 5 mmol alpha bromo acetophenone derivatives (**15k–t**) to the reaction medium. As the reaction progressed, solid particles began to form, and the reaction was terminated. The reaction mixture, which was cooled to room temperature, was transferred to 50 ml of ice-water mixture and magnetically stirred for 30 min. The solid particles formed were separated by filtration, washed in 15 ml of an ethanol-water mixture (1:1), and dried in an oven at 40 °C. The obtained thiazole hydrazone derivatives (**16a–t**) were used in the next step without further purification.[26]

**Table 5.** Predicted toxicities and some ADME properties of Celecoxib and hit compounds.

| | Celecoxib | 19d | 19e | 19l | 19m |
|---|---|---|---|---|---|
| **hERG Blockers** | – | — | — | — | — |
| **H-HT** | + | – | – | ++ | ++ |
| **FDAMDD** | + | – | – | ++ | ++ |
| **HIA** | — | — | — | — | — |
| **PPB (%)** | 94.96 | 98.54 | 98.43 | 100 | 100 |
| **CYP2C9 inhibitor** | ++ | ++ | +++ | +++ | +++ |
| **CL** | 0.99 | 5.35 | 6.56 | 6.26 | 5.06 |
| **Lipinski Rule** | Accepted | Accepted | Accepted | Accepted | Accepted |

**Synthesis of compounds 17 a–t**. A chilled solution of 3 mmol *N, N*-dimethyl formamide (DMF), and 3 mmol $POCl_3$ was added dropwise on each other and stirred for 15 min at 0 °C. A solution of 1 mmol thiazole hydrazone derivatives (**16 a–t**) in DMF (3 mL) was added dropwise to the reaction mixture and heated at 80 °C for 6 h. The reaction mixture was cooled to room temperature, transferred to 20 ml of an ice-water mixture, and stirred for 30 min. Then, 10% aqueous sodium hydroxide (NaOH) solution was added dropwise to the reaction mixture until pH 8. The resulting precipitate was filtered, washed with water (15 mL), and dried in the open air. The crude products (**17 a–t**) were purified by column chromatography on silica gel eluting with n-hexane/EtOAc (5/1).[26]

**Synthesis of final compounds 19 a–t**. To a solution of compounds **17 a–t** (1 mol) in n-PrOH (5 mL) was added $NH_2OH$-HCl (1.2 mol) portionwise at room temperature for 10 min. The resulting mixture was refluxed at 90 °C for 3 hours and the formation of oxime derivatives (**18 a–t**) was observed under TLC control.[31] Before the reaction was terminated, acetic anhydride (2 mL) was added dropwise into the reaction flask. The reaction mixture was refluxed for an additional 2 h., and after the completion of time, the reaction was terminated and cooled to room temperature. After adding water (50 mL), the mixture was extracted with EtOAc (4×25 mL). The extracts were washed with brine (6×15 mL), dried over $MgSO_4$, and evaporated. The crude products (**19 a-t**) were purified by chromatography on silica gel eluting with hexane/EtOAc (5 : 1).[32] The structure of newly synthesized compounds was elucidated based on elemental analysis and spectral data. The physical properties and spectral data of the compounds are presented below.

**3-Phenyl-1-(4-phenylthiazol-2-yl)-1*H*-pyrazole-4-carbonitrile (*19 a*)**. White solid, M.p. 177–178 °C, Yield: 87%. $^1$H NMR (400 MHz, $CDCl_3$) δ 8.91 (s, 1H, Ar–H), 8.10–8.07 (m, 2H, Ar–H), 7.92–7.88 (m, 2H, Ar–H), 7.55–7.49 (m, 3H, Ar–H), 7.49–7.44 (m, 2H, Ar–H), 7.42–7.38 (m, 1H, Ar–H), 7.37 (s, 1H, Ar–H). $^{13}$C NMR (100 MHz, $CDCl_3$) δ 159.0, 154.7, 153.2, 133.8, 133.4, 130.2, 129.4, 129.0, 128.9, 128.8, 127.0, 126.1, 113.5, 110.8, 93.1. Anal. calc. for $C_{19}H_{12}N_4S$: C: 69.49; H: 3.68; N: 17.06; Found: C: 69.52; H: 3.65; N: 17.11.

**1-(4-Phenylthiazol-2-yl)-3-(p–tolyl)-1*H*-pyrazole-4-carbonitrile (*19 b*)**. Light yellow powder, M.p. 155–156 °C, Yield: 89%. $^1$H NMR (400 MHz, $CDCl_3$) δ 8.88 (s, 1H, Ar–H), 8.00–7.94 (m, AA'BB' system, 2H, Ar–H), 7.93–7.87 (m, 2H, Ar–H), 7.49–7.43 (m, 2H, Ar–H), 7.42–7.37 (m, 1H, Ar–H), 7.36 (s, 1H, Ar–H), 7.34–7.29 (m, AA'BB' system, 2H, Ar–H), 2.43 (s, 3H, $-CH_3$). $^{13}$C NMR (100 MHz, $CDCl_3$) δ 159.0, 154.7, 153.1, 140.5, 133.7, 133.4, 129.7, 128.8, 128.7, 126.9, 126.7, 126.1, 113.6, 110.7, 92.9, 21.5. Anal. calc. for $C_{20}H_{14}N_4S$: C: 70.15; H: 4.12; N: 16.36; Found: C: 70.21; H: 4.07; N: 16.30.

**3-(4-Hydroxyphenyl)-1-(4-phenylthiazol-2-yl)-1*H*-pyrazole-4-carbonitrile (*19 c*)**. Gray powder, M.p. 205–206 °C, Yield: 73%. $^1$H NMR (400 MHz, $CDCl_3$) δ 8.90 (s, 1H, Ar–H), 8.13–8.09 (m, AA'BB' system, 2H, Ar–H), 7.92–7.88 (m, 2H, Ar–H), 7.49–7.44 (m, 2H, Ar–H), 7.42–7.36 (m, 2H, Ar–H), 7.26–7.23 (m, AA'BB' system, 2H, Ar–H), 2.34 (s, 1H, –OH). $^{13}$C NMR (100 MHz, $CDCl_3$) δ 169.1, 158.9, 153.7, 153.2, 152.1, 133.8, 133.3, 128.9, 128.2, 127.1, 126.1, 122.3, 113.4, 110.9, 92.9. Anal. calc. for $C_{19}H_{12}N_4OS$: C: 66.26; H: 3.51; N: 16.26; Found: C: 66.31; H: 3.45; N: 16.24.

**3-(4-Methoxyphenyl)-1-(4-phenylthiazol-2-yl)-1*H*-pyrazole-4-carbonitrile (*19 d*)**. Light yellow powder, M.p. 197–198 °C, Yield: 86%. $^1$H NMR (400 MHz, $CDCl_3$) δ 8.86 (s, 1H, Ar–H), 8.06–8.00 (m, AA'BB' system, 2H, Ar–H), 7.92–7.87 (m, 2H, Ar–H), 7.49–7.43 (m, 2H, Ar–H), 7.41–7.36 (m, 1H, Ar–H), 7.35 (s, 1H, Ar–H), 7.05–6.99 (m, AA'BB' system, 2H, Ar–H), 3.88 (s, 3H, –OMe). $^{13}$C NMR (100 MHz, $CDCl_3$) δ 161.1, 159.1, 154.5, 153.1, 133.7, 133.4, 128.9, 128.7, 128.5, 126.1, 122.1, 114.4, 113.7, 110.7, 92.6, 55.4. Anal. calc. for $C_{20}H_{14}N_4OS$: C: 67.02; H: 3.94; N: 15.63; Found: C: 66.98; H: 3.89; N: 15.66.

**3-(3,4-Dimethoxyphenyl)-1-(4-phenylthiazol-2-yl)-1*H*-pyrazole-4-carbonitrile (*19 e*)**. Dark orange powder, M.p. 136–137 °C, Yield: 85%. $^1$H NMR (400 MHz, $CDCl_3$) δ 8.87 (s, 1H, Ar–H), 7.92–7.87 (m, 2H, Ar–H), 7.70 (dd, $J$ = 2.1 Hz, $J$ = 8.4 Hz, 1H, Ar–H), 7.60 (d, $J$ = 2.1 Hz, 1H, Ar–H), 7.48–7.44 (m, 2H, Ar–H), 7.41–7.37 (m, 1H, Ar–H), 7.36 (s, 1H, Ar–H), 6.98 (d, $J$ = 8.4 Hz, 1H, Ar–H), 4.00 (s, 3H, –OMe), 3.95 (s, 3H, –OMe). $^{13}$C NMR (100 MHz, $CDCl_3$) δ 159.0, 154.5, 153.1, 150.7, 149.2, 133.7, 133.4, 128.9, 128.8, 126.1, 122.2, 120.1, 113.8, 111.2, 110.7, 109.6, 92.7, 56.1, 56.0. Anal. calc. for $C_{21}H_{16}N_4O_2S$: C: 64.93; H: 4.15; N: 14.42; Found: C: 64.99; H: 4.09; N: 14.45.

**3-(4-Fluorophenyl)-1-(4-phenylthiazol-2-yl)-1*H*-pyrazole-4-carbonitrile (*19 f*)**. Light gray powder, M.p. 163–164 °C, Yield: 73%. $^1$H NMR (400 MHz, $CDCl_3$) δ 8.91 (s, 1H, Ar–H), 8.11–8.06 (m, AA'BB' system, 2H, Ar–H), 7.92-7.87 (m, 2H, Ar–H), 7.50–7.44 (m, 2H, Ar–H), 7.43–7.36 (m, 2H, Ar–H), 7.24–7.18 (m, 2H, Ar–H). $^{13}$C NMR (100 MHz, $CDCl_3$) δ 165.1, 162.6, 153.7, 153.2, 133.8, 133.7, 133.3, 129.1, 129.0, 126.1, 116.3, 116.0, 113.4, 110.9, 92.9. Anal. calc. for $C_{19}H_{11}FN_4S$: C: 65.88; H: 3.20; N: 16.18; Found: C: 65.93; H: 3.15; N: 16.21.

**1-(4-Phenylthiazol-2-yl)-3-(4-(trifluoromethyl)phenyl)-1*H*-pyrazole-4-carbonitrile (*19 g*)**. Light yellow powder, M.p. 196–197 °C, Yield: 83%. $^1$H NMR (400 MHz, $CDCl_3$) δ 8.94 (s, 1H, Ar–H), 8.23–8.18 (m, AA'BB' system, 2H, Ar–H), 7.93–7.87 (m, 2H, Ar–H), 7.81–7.75 (m, AA'BB' system, 2H, Ar–H), 7.50–7.44 (m, 2H, Ar–H), 7.42–7.38 (m, 2H, Ar–H). $^{13}$C NMR (100 MHz, $CDCl_3$) δ 158.7, 153.3, 153.1, 134.0, 133.9, 133.2, 132.8, 132.1, 128.9, 127.3, 126.2, 126.1, 113.1, 111.1, 111.0, 93.3. Anal. calc. for $C_{20}H_{11}F_3N_4S$: C: 60.60; H: 2.80; N: 14.13; Found: C: 60.56; H: 2.84; N: 14.19.

**1-(4-Phenylthiazol-2-yl)-3-(thiophen-2-yl)-1*H*-pyrazole-4-carbonitrile (*19 h*)**. Light yellow powder, M.p. 79–80 °C, Yield: 97%. $^1$H NMR (400 MHz, $CDCl_3$) δ 8.85 (s, 1H, Ar–H), 7.93–7.87 (m, 3H, Ar–H), 7.48–7.44 (m, 3H, Ar–H), 7.42–7.38 (m, 1H, Ar–H), 7.37 (s, 1H, Ar–H), 7.17 (dd, $J$ = 3.7 Hz, $J$ = 5.1 Hz, 1H, Ar–H). $^{13}$C NMR (100 MHz, $CDCl_3$) δ 158.7, 153.1, 150.0, 133.4, 133.3, 131.5, 128.9, 128.7, 128.1, 127.9, 126.1, 113.0, 110.9, 110.8, 92.4. Anal. calc. for $C_{17}H_{10}N_4S_2$: C: 61.06; H: 3.01; N: 16.75; Found: C: 61.12; H: 3.04; N: 16.80.

**3-(Naphthalen-2-yl)-1-(4-phenylthiazol-2-yl)-1*H*-pyrazole-4-carbonitrile (*19 i*)**. Brown solid, M.p. 267–268 °C, Yield: 88%. $^1$H NMR (400 MHz, $CDCl_3$) δ 8.93 (s, 1H, Ar–H), 8.60 (d, $J$ = 0.9 Hz, 1H, Ar–H), 8.16 (dd, $J$ = 1.8 Hz, $J$ = 8.6 Hz, 1H, Ar–H), 8.00–7.95 (m, 2H, Ar–H), 7.93–7.87 (m, 3H, Ar–H), 7.58–7.53 (m, 2H, Ar–H), 7.50–7.44 (m, 2H, Ar–H), 7.43–7.36 (m, 2H, Ar–H). $^{13}$C NMR (100 MHz, $CDCl_3$) δ 159.0, 154.5, 153.2, 133.9, 133.8, 133.4, 133.1, 128.8, 127.8, 127.7, 127.3, 127.2, 126.8, 126.7, 126.2, 126.1, 123.9, 113.6, 110.9, 110.7, 93.1. Anal. calc. for $C_{23}H_{14}N_4S$: C: 73.00; H: 3.73; N: 14.80; Found: C: 73.05; H: 3.71; N: 14.76.

**3-([1,1′-Biphenyl]-4-yl)-1-(4-phenylthiazol-2-yl)-1*H*-pyrazole-4-carbonitrile (*19 j*)**. Light gray powder, M.p. 216–218 °C, Yield: 91%. $^1$H NMR (400 MHz, $CDCl_3$) δ 8.91 (s, 1H, Ar–H), 8.19–8.14 (m, 2H, Ar–H), 7.94–7.88 (m, 2H, Ar–H), 7.77–7.72 (m, 2H, Ar–H), 7.68–7.63 (m, 2H, Ar–H), 7.51–7.44 (m, 4H, Ar–H), 7.43–7.39 (m, 2H, Ar–H), 7.38 (s, 1H, Ar–H). $^{13}$C NMR (100 MHz, $CDCl_3$) δ 159.0, 154.3, 153.2, 149.7, 142.9, 140.2, 133.8, 133.4, 128.9, 128.3, 127.9, 127.7, 127.4, 127.1, 126.1, 113.5, 110.8, 110.7, 93.0. Anal. calc. for $C_{25}H_{16}N_4S$: C: 74.24; H: 3.99; N: 13.85; Found: C: 74.29; H: 4.04; N: 13.91.

**3-Phenyl-1-(4-(p–tolyl)thiazol-2-yl)-1*H*-pyrazole-4-carbonitrile (*19 k*)**. Light orange solid, M.p. 177–178 °C, Yield: 78%. $^1$H NMR (400 MHz, $CDCl_3$) δ 8.87 (s, 1H, Ar–H), 8.11–8.00 (m, 3H, Ar–H), 7.79–7.76 (m, 1H, Ar–H), 7.55–7.48 (m, 3H, Ar–H), 7.35–7.24 (m, 3H, Ar–H), 2.40 (s, 3H, $-CH_3$). $^{13}$C NMR (100 MHz, $CDCl_3$) δ 158.9, 154.7, 153.3, 138.8, 133.8, 130.7, 130.2, 129.6, 129.5, 129.0, 127.0, 126.1,

113.5, 110.0, 93.0, 21.3. Anal. calc. for $C_{20}H_{14}N_4S$: C: 70.15; H: 4.12; N: 16.36; Found: C: 70.19; H: 4.17; N: 16.41.

**1-(4-(4-Methoxyphenyl)thiazol-2-yl)-3-phenyl-1*H*-pyrazole-4-carbonitrile (*19l*)**. Light yellow solid, M.p. 148–149 °C, Yield: 76%. $^1$H NMR (400 MHz, $CDCl_3$) δ 8.88 (s, 1H, Ar–H), 8.13–8.05 (m, 2H, Ar–H), 7.85–7.79 (m, AA'BB' system, 2H, Ar–H), 7.55–7.48 (m, 3H, Ar–H), 7.22 (s, 1H, Ar–H), 7.05–6.95 (m, AA'BB' system, 2H, Ar–H), 3.86 (s, 3H, –OMe). $^{13}$C NMR (100 MHz, $CDCl_3$) δ 160.1, 154.6, 152.9, 133.8, 129.5, 128.9, 127.5, 127.0, 126.3, 114.2, 113.5, 112.8, 109.0, 108.8, 92.9, 55.3. Anal. calc. for $C_{20}H_{14}N_4OS$: C: 67.02; H: 3.94; N: 15.63; Found: C: 66.96; H: 4.02; N: 15.66.

**1-(4-(4-Chlorophenyl)thiazol-2-yl)-3-phenyl-1*H*-pyrazole-4-carbonitrile (*19m*)**. Light brown powder, M.p. 275–276 °C, Yield: 97%. $^1$H NMR (400 MHz, $CDCl_3$) δ 8.90 (s, 1H, Ar–H), 8.10–8.06 (m, 2H, Ar–H), 7.85–7.82 (m, AA'BB' system, 2H, Ar–H), 7.54–7.49 (m, 3H, Ar–H), 7.45–7.41 (m, AA'BB' system, 2H, Ar–H), 7.36 (s, 1H, Ar–H). $^{13}$C NMR (100 MHz, $CDCl_3$) δ 154.7, 152.0, 134.6, 133.8, 131.8, 130.3, 129.4, 129.1, 129.0, 127.3, 127.0, 113.4, 111.2, 111.0, 93.2. Anal. calc. for $C_{19}H_{11}ClN_4S$: C: 62.90; H: 3.06; N: 15.44; Found: C: 62.94; H: 3.11; N: 15.49.

**1-(4-(3,4-Dichlorophenyl)thiazol-2-yl)-3-phenyl-1*H*-pyrazole-4-carbonitrile (*19n*)**. Light brown powder, M.p. 241–242 °C, Yield: 93%. $^1$H NMR (400 MHz, $CDCl_3$) δ 8.90 (s, 1H, Ar–H), 8.10–8.06 (m, 2H, Ar–H), 8.01 (d, $J$ = 2.1 Hz, 1H, Ar–H), 7.71 (dd, $J$ = 8.4 Hz, $J$ = 2.1 Hz, 1H, Ar–H), 7.75–7.49 (m, 4H, Ar–H), 7.39 (s, 1H, Ar–H). $^{13}$C NMR (100 MHz, $CDCl_3$) δ 154.8, 150.7, 133.9, 133.7, 133.2, 132.7, 129.3, 129.2, 129.0, 128.1, 128.0, 127.0, 126.9, 113.3, 112.1, 111.9, 93.4. Anal. calc. for $C_{19}H_{10}C_{l2}N_4S$: C: 57.44; H: 2.54; N: 14.10; Found: C: 57.39; H: 2.58; N: 14.05.

**1-(4-(4-bromophenyl)thiazol-2-yl)-3-phenyl-1*H*-pyrazole-4-carbonitrile (*19o*)**. Gray powder, M.p. 214–215 °C, Yield: 79%. $^1$H NMR (400 MHz, $CDCl_3$) δ 8.89 (s, 1H, Ar–H), 8.10–8.06 (m, 2H, Ar–H), 7.78–7.74 (m, AA'BB' system, 2H, Ar–H), 7.61–7.55 (m, AA'BB' system, 2H, Ar–H), 7.54–7.49 (m, 3H, Ar–H), 7.37 (s, 1H, Ar–H). $^{13}$C NMR (100 MHz, $CDCl_3$) δ 159.2, 154.7, 152.0, 133.7, 132.3, 132.1, 130.3, 129.3, 129.1, 127.7, 127.0, 122.8, 113.4, 111.1, 93.2. Anal. calc. for $C_{19}H_{11}BrN_4S$: C: 56.03; H: 2.72; N: 13.76; Found: C: 56.05; H: 2.79; N: 13.82.

**3-phenyl-1-(4-(4-(trifluoromethyl)phenyl)thiazol-2-yl)-1*H*-pyrazole-4-carbonitrile (*19p*)**. Light brown powder, M.p. 180–181 °C, Yield: 80%. $^1$H NMR (400 MHz, $CDCl_3$) δ 8.91 (s, 1H, Ar–H), 8.11–8.07 (m, 2H, Ar–H), 8.04–7.97 (m, AA'BB' system, 2H, Ar–H), 7.75–7.68 (m, AA'BB' system, 2H, Ar–H), 7.54–7.46 (m, 4H, Ar–H). $^{13}$C NMR (100 MHz, $CDCl_3$) δ 159.4, 154.8, 151.6, 136.5, 133.8, 130.3, 129.3, 129.1, 129.0, 127.0, 126.3, 125.9, 113.3, 112.7, 112.6, 93.3. Anal. calc. for $C_{20}H_{11}F_3N_4S$: C: 60.60; H: 2.80; N: 14.13; Found: C: 60.66; H: 2.83; N: 14.08.

**1-(4-(4-nitrophenyl)thiazol-2-yl)-3-phenyl-1*H*-pyrazole-4-carbonitrile (*19r*)**. Brown powder, M.p. 227–228 °C, Yield: 74%. $^1$H NMR (400 MHz, $d_6$-DMSO) δ 9.66 (s, 1H, Ar–H), 8.43 (s, 1H, Ar–H), 8.37–8.32 (m, AA'BB' system, 2H, Ar–H), 8.29–8.24 (m, AA'BB' system, 2H, Ar–H), 7.97–7.93 (m, 2H, Ar–H), 7.63–7.55 (m, 3H, Ar–H). $^{13}$C NMR (100 MHz, $d_6$-DMSO) δ 159.8, 154.4, 149.8, 147.5, 139.5, 136.9, 129.7, 129.5, 127.4, 127.2, 124.8, 117.9, 114.0, 93.1. Anal. calc. for $C_{19}H_{11}N_5O_2S$: C: 61.12; H: 2.97; N: 18.76; Found: C: 61.18; H: 3.01; N: 18.81.

**1-(4-(Naphthalen-2-yl)thiazol-2-yl)-3-phenyl-1*H*-pyrazole-4-carbonitrile (*19s*)**. Dark brown solid, M.p. 156–157 °C, Yield: 84%. $^1$H NMR (400 MHz, $CDCl_3$) δ 8.93 (s, 1H, Ar–H), 8.41 (bs, 1H, Ar–H), 8.11–8.05 (m, 2H, Ar–H), 7.97–7.84 (m, 4H, Ar–H), 7.58–7.49 (m, 5H, Ar–H), 7.46 (s, 1H, Ar–H). $^{13}$C NMR (100 MHz, $CDCl_3$) δ 160.9, 159.0, 154.6, 153.0, 133.7, 133.4, 130.6, 130.2, 129.4, 129.1, 129.0, 128.5, 127.8, 127.0, 126.6, 125.4, 123.6, 113.5, 111.2, 111.0, 93.0. Anal. calc. for $C_{23}H_{14}N_4S$: C: 73.00; H: 3.73; N: 14.80; Found: C: 73.06; H: 3.69; N: 14.83.

**1-(4-([1,1′-Biphenyl]-4-yl)thiazol-2-yl)-3-phenyl-1*H*-pyrazole-4-carbonitrile (*19t*)**. Dark brown powder, M.p. 187–188 °C, Yield: 82%. $^1$H NMR (400 MHz, $CDCl_3$) δ 8.92 (s, 1H, Ar–H), 8.13–8.05 (m, 2H, Ar–H), 8.01–7.91 (m, AA'BB' system, 2H, Ar–H), 7.72–7.62 (m, 4H, Ar–H), 7.54–7.46 (m, 5H, Ar–H), 7.42–7.36 (m, 2H, Ar–H). $^{13}$C NMR (100 MHz, $CDCl_3$) δ 159.0, 154.7, 152.8, 141.4, 140.3, 133.8, 132.3, 129.4, 129.1, 129.0, 128.8, 127.6, 127.5, 126.9, 126.6, 113.5, 110.8, 110.7, 93.0. Anal. calc. for $C_{25}H_{16}N_4S$: C: 74.24; H: 3.99; N: 13.85; Found: C: 74.16; H: 4.04; N: 13.90.

## Biology

**Cell Viability Assay**. The cell viability was assessed by the MTT method described by Razak et al. (2019)[33] with some modifications. MDA-MB-231 or NIH/3T3 cells were seeded in a 96-well plate at $6\times10^3$ cells per well, then allowed to attach for 24 h at 37 °C, 5% $CO_2$. Briefly, the compounds, Celecoxib and doxorubicin (as a positive control, data not shown in Table 1) were dissolved in DMSO. Then the cells ($6\times10^3$) were treated with various concentrations (12, 25, 50, 100, 250, and 500 μM) of the compounds and Celecoxib for 24 h after attachment. The maximum DMSO concentration did not exceed 1%. After incubation, the medium was discarded, and a new medium containing MTT solution (1 mg/mL in final concentration) was added and incubated for an extra 4 h. Subsequently, all media were discarded at the end of the incubation, and formazan crystals were dissolved in 150 μL of DMSO. The absorbance values were measured at 550 nm. Cytotoxic doses ($IC_{50}$) that killed 50% of cells were calculated using GraphPad Prism. Moreover, the degree of selectivity of the cytotoxic compounds was expressed as SI = $IC_{50}$ in healthy cells/$IC_{50}$ in breast cancer cells.

**Inhibitory Activity of the Compounds on Human COX-1 and COX-2**. The potential activity of the compounds and Celecoxib on COX enzymes was evaluated by the COX Activity Assay Kit (Fluorometric) (Abcam, ab204699) according to the manufacturer's instructions on the cell lysates. The cells were incubated for 24 h with various concentrations (1, 12, 25, 50, 100, 250, 500, 750 μM) of the compounds. At the end of the incubation, the cells were trypsinized and lysed with the 300 μl RIPA buffer containing a 1% protease inhibitor cocktail. After centrifugation (12000 xg for 3 min), the supernatants were separated to measure COX enzyme activity. For COX-1 and COX-2 inhibition activities, 20 μL of reaction buffer containing cell lysate and 68 μL of reaction mix (2 μL COX probe 2, 4 μL diluted COX cofactor, and 130 μL COX assay buffer) were placed on a 96-well plate. 2 μL COX-1 Inhibitor (SC560) or COX-2 Inhibitor (Celecoxib) were added to wells to measure the specific COX-1 or COX-2 activities. The enzymatic reaction produced a fluorescent molecule (resorufin dye, Ex/Em = 535/587 nm) with the addition of arachidonic acid (COX substrate) in NaOH solution, which could be measured in kinetic mode for 30 min at room temperature.[34] The $IC_{50}$ value of COX-1 or COX-2 for each compound was determined with GraphPad Prism. The COX-2 selectivity of the compounds was also calculated according to the formula in parentheses: [COX-2 enzyme selective inhibition = $IC_{50}$ (COX-1)/$IC_{50}$ (COX-2).]

**Pharmacokinetic calculations**. Some toxicities and ADME properties of the hit compounds and Celecoxib were evaluated by ADMETlab 2.0, which is composed of a series of high-quality prediction models trained by the multi-task graph attention framework.[35] SMILES of the compounds were generated by pkCSM

online server and SMILES of Celecoxib were obtained from PubChem and used in the ADMETlab web tool for the predictions.

## Supporting Information

The Supporting Information contains $^{1}$H- and $^{13}$C-NMR spectrums of compounds 19a-t.

## Acknowledgements

This study was funded by Scientific and Technologic Research Agency of Turkey (TÜBİTAK) (grant number: 223S065).

## Conflict of Interests

The authors declare no conflict of interest.

## Data Availability Statement

The data that support the findings of this study are available from the corresponding author upon reasonable request.

**Keywords:** Thiazolyl-pyrazole · COX-2 inhibition · Molecular docking · ADMET · SAR

[1] J. C. Otto, W. L. Smith, *Adv. Prostaglandin Thromboxane Leukotriene Res.* **1995**, *23*, 29.
[2] T. Miller, *Am. J. Physiol. Gastrointest. Liver Physiol.* **1983**, *245(5)*, 601.
[3] B. Hinz, K. Brune, *J. Pharmacol. Exp. Ther.* **2002**, *300(2)*, 367.
[4] N. V. Chandrasekharan, H. Dai, K. L. T. Roos, N. K. Evanson, J. Tomsik, T. S. Elton, D. L. Simmons, *Proc. Nat. Acad. Sci.* **2002**, *99(21)*, 13926.
[5] A. K. Gupta, R. A. Gupta, L. K. Soni, S. G. Kaskhedikar, *Eur. J. Med. Chem.* **2008**, *43(6)*, 1297.
[6] A. Tanaka, H. Araki, Y. Komoike, S. Hase, K. Takeuchi, *J. Physiol.* **2001**, *95(1–6)*, 21.
[7] M. M. Ahlström, M. Ridderström, I. Zamora, K. Luthman, *J. Med. Chem.* **2007**, *50(18)*, 4444.
[8] J. L. Wallace, W. McKnight, B. K. Reuter, N. Vergnolle, *Gastroenterology.* **2000**, *119(3)*, 706.
[9] P. F. Lamie, W. A. Ali, V. Bazgier, L. Rárová, *Eur. J. Med. Chem.* **2016**, *123*, 803.
[10] C. Charlier, C. Michaux, *Eur. J. Med. Chem.* **2003**, *38(7–8)*, 645.
[11] C. H. Lou, C. P. Morris, J. Sachithanandham, A. Amadi, D. C. Gaston, M. Li, N. J. Swanson, M. Schwartz, E. Y. Klein, A. Pekosz, H. H. Mostafa, *Clin. Infect. Dis.* **2022**, *75(1)*, 715.
[12] Z. Zhu, X. Lian, X. Su, W. Wu, G. A. Marraro, Y. Zeng, *Respir. Res.* **2020**, *21(1)*, 1.
[13] Z. Abdelrahman, M. Li, X. Wang, *Front. Immunol.* **2020**, *11*, 552909.
[14] L. Chen, H. Deng, H. Cui, J. Fang, Z. Zuo, J. Deng, *Oncotarget.* **2018**, *9(6)*, 7204.
[15] N. Chandna, S. Kumar, P. Kaushik, D. Kaushik, S. K. Roy, G. K. Gupta, P. K. Sharma, *Bioorg. Med. Chem.* **2013**, *21(15)*, 4581.
[16] K. R. Abdellatif, M. A. Abdelgawad, M. B. Labib, T. H. Zidan, *Arch. Pharm.* **2017**, *350(8)*, 1600386.
[17] E. K. Abdelall, G. M. Kamel, *Eur. J. Med. Chem.* **2016**, *118*, 250–258.
[18] H. A. Abd El Razik, M. H. Badr, A. H. Atta, S. M. Mouneir, M. M. Abu-Serie, *Arch. Pharm.* **2017**, *350(5)*, 1700026.
[19] A. A. Magda, N. I. Abdel-Aziz, A. M. Alaa, A. S. El-Azab, K. E. ElTahir, *Bioorg. Med. Chem.* **2012**, *20(10)*, 3306.
[20] K. R. Abdellatif, W. A. Fadaly, Y. A. Elshaier, W. A. Ali, G. M. Kamel, *Bioorg. Chem.* **2018**, *77*, 568.
[21] M. S. El-Shoukrofy, H. A. Abd El Razik, O. M. AboulWafa, A. E. Bayad, I. M. El-Ashmawy, *Bioorg. Chem.* **2019**, *85*, 541–557.
[22] S. G. Alegaon, K. R. Alagawadi, M. K. Garg, K. Dushyant, D. Vinod, *Bioorg. Chem.* **2014**, *54*, 51.
[23] N. Inceler, Y. Ozkan, N. N. Turan, D. C. Kahraman, R. Cetin-Atalay, S. N. Baytas, *MedChemComm.* **2018**, *9(5)*, 795.
[24] G. N. Tageldin, S. M. Fahmy, H. M. Ashour, M. A. Khalil, R. A. Nassra, I. M. Labouta, *Bioorg. Chem.* **2018**, *78*, 358–371.
[25] E. S. Nossier, H. H. Fahmy, N. M. Khalifa, W. I. El-Eraky, M. A. Baset, *Molecules.* **2017**, *22(4)*, 512.
[26] B. Kuzu, A. Ergüç, F. Karakuş, E. Arzuk, *Med. Chem. Res.* **2023**, *32*, 1690–1700.
[27] Z. J. Dai, X. B. Ma, H. F. Kang, J. Gao, W. L. Min, H. T. Guan, Y. Diao, W. F. Lu, X. J. Wang, *Cancer Cell Int.* **2012**, *12(1)*, 53.
[28] Z. Ju, Z. Shang, T. Mahmud, J. Fang, Y. Liu, Q. Pan, X. Lin, F. Chen, *J. Nat. Prod.* **2023**, *86(4)*, 958.
[29] L. Gong, C. F. Thorn, M. M. Bertagnolli, T. Grosser, R. B. Altman, T. E. Klein, *Pharmacogenet. Genomics.* **2012**, *22(4)*, 310.
[30] E. Kuzu, B. Kuzu, *Chem. Heterocycl. Compd.* **2023**, *59(1–2)*, 80.
[31] B. Kuzu, M. Tan, Z. Ekmekci, N. Menges, *J. Lumin.* **2017**, *192*, 1096.
[32] Y. She, Y. Lu, C. Jia, Y. Li, Y. Q. Yao, *New J. Chem.* **2023**, *47(33)*, 15650.
[33] N. A. Razak, N. Abu, W. Y. Ho, N. R. Zamberi, S. W. Tan, N. B. Alitheen, K. Long, S. K. Yeap, *Sci. Rep.* **2019**, *9(1)*, 1514.
[34] E. Mauri, A. Rossetti, P. Mozetic, C. Schiavon, A. Sacchetti, A. Rainer, F. Rossi, *Eur. J. Pharm. Biopharm.* **2020**, *146*, 143–149.
[35] G. Xiong, Z. Wu, J. Yi, L. Fu, Z. Yang, C. Hsieh, M. Yin, X. Zeng, C. Wu, A. Lu, X. Chen, T. Hou, D. Cao, *Nucleic Acids Res.* **2021**, *49(W1)*, W5.

Manuscript received: November 29, 2023